AIP | Journal of Applied Physics

Nuclear spin depolarization via slow spin diffusion in single InAlAs quantum dots observed by using erase-pump-probe technique

S. Adachi, R. Kaji, S. Furukawa, Y. Yokoyama, and S. Muto

Citation: J. Appl. Phys. **111**, 103531 (2012); doi: 10.1063/1.4721902
View online: http://dx.doi.org/10.1063/1.4721902
View Table of Contents: http://jap.aip.org/resource/1/JAPIAU/v111/i10
Published by the American Institute of Physics.

Nuclear spin depolarization via slow spin diffusion in single InAlAs quantum dots observed by using erase-pump-probe technique

S. Adachi,[a] R. Kaji, S. Furukawa, Y. Yokoyama, and S. Muto
Department of Applied Physics, Hokkaido University, Sapporo 060-8628, Japan

(Received 8 February 2012; accepted 1 May 2012; published online 30 May 2012)

Nuclear spin diffusion in single self-assembled InAlAs quantum dots was studied by using erase-pump-probe technique. As a measure of nuclear spin polarization, transients of the Overhauser shift (OHS) of positive trion were probed in the respective pulse region. The achieved stable OHS was relaxed with a long depolarization time as long as a few tens of seconds and a diffusion constant of $\sim 5 \times 10^{-15}$ cm^2/s was estimated. The slow transfer of the spin energy is considered to be due to the dipole-dipole interaction of the nuclei. In addition, through the magnetic field dependence of OHS, the stability of the nuclear spin polarization was briefly discussed, and the saturated maximum values of OHS were investigated experimentally. © *2012 American Institute of Physics*. [http://dx.doi.org/10.1063/1.4721902]

I. INTRODUCTION

Recently, studies on localized spins have been attracting a lot of interests. One of the central topics is the spin interaction between a localized electron and nuclei, which comes into focus in the field of single electron spin manipulation in semiconductor nanostructures. Since the localization suppresses significantly the electron spin relaxation mechanism based on the spin-orbit interaction, an electron can interact strongly with nuclei in the wave function for a long time, and the interaction (Fermi's contact term of hyperfine interaction) makes a large nuclear spin polarization (NSP) via mutual spin flip (i.e., flip-flop) process. The averaged NSP $\langle I_z \rangle$ acts back on the spin-unpaired electrons as an effective magnetic field (Overhauser field) B_N and induces the spin-dependent energy shift of the electronic states (Overhauser shift: OHS).[1,2] Since, with the localized electrons, the nuclear spins show the distinctive nonlinear response "bistability" to the externally controllable parameters, the interaction can offer a powerful tool to change the electron spin properties. In particular, semiconductor quantum dots (QDs) serve the advantageous platform in order to utilize this interaction because of the strong confinement and the controllability of an electron.

Beginning with the first observation of large B_N in a single interface GaAs QD (Ref. 3) and a single self-assembled InAlAs QDs,[4] research of the NSP in QDs has progressed fast, and the *nuclear spin switching* (bistable response) was also observed in self-assembled InGaAs QDs,[5–7] InAlAs QDs,[8,9] and InP QDs.[10] These studies open the way to the fascinating applications of NSP in QDs such as quantum memory[11] and conversion between electron spin qubit and photon qubit.[12] In these applications, the precise control of single electron spins in QDs is necessary to achieve a high degree of control of nuclear spin ensemble via the hyperfine interaction. Although several works were devoted to the study of electron-nuclear spin dynamics in various QD materials, the details including the nuclear spin polarization and depolarization processes are still unclear, and the data have to be accumulated in various QD materials. In particular, the nuclear spin depolarization, which is the decay of the longitudinal component of averaged NSP in the QD region, is the main process to limit the permanence of nuclear spin memory. Accordingly, the measurements and investigation of the nuclear spin depolarization time are very important.

In this study, nuclear spin depolarization in single self-assembled InAlAs QDs was studied by using an erase-pump-probe technique. Transients of the OHS of positive trion were probed as a measure of NSP. The stability of the high NSP state was discussed first, which was found to be preferable as an initial state for the NSP decay measurement. The created stable NSP was relaxed with a long depolarization time as long as a few tens of seconds, and by using a standard three dimensional diffusion model, the diffusion constant of $\sim 5 \times 10^{-15}$ cm^2/s was estimated. The observed slow transfer of the spin energy under no electron in a QD is considered to be due to a dipole-dipole interaction between the nuclear spins. In addition, the pump duration dependence of the transients suggests that the NSP created during the pump duration in the surrounding barrier material suppresses strongly the nuclear spin diffusion from a QD region.

II. EXPERIMENTS

Self-assembled $In_{0.75}Al_{0.25}$ As QDs were used for the experiments. The QDs were embedded with $Al_{0.3}Ga_{0.7}$ As layers grown on an undoped (100) GaAs substrate in the Stranski-Krastanov growth mode by molecular beam epitaxy. The average diameter, height, and density of the QDs were found to be $\sim$20 nm, $\sim$4 nm, and $\sim 5 \times 10^{10}$ cm^{-2}, respectively, by the atomic force microscopy measurements on a reference uncapped QD sample with the same growth conditions. Assuming the lens shaped QD based on the cross-section transmission electron microscope observation, the number of nuclei in a single QD is estimated roughly to be $\sim 3 \times 10^4$.

[a]Electronic mail: adachi-s@eng.hokudai.ac.jp.

After the fabrication of small mesa structures (top lateral diameter ~150 nm), the micro-photoluminescence (μ-PL) measurements in the time-integrated and/or time-resolved modes were performed at 6 K under a longitudinal magnetic field (B_z) of up to 5 T. A cw Ti:sapphire laser of ~728 nm, which provides the transition energy to the wetting layer of InAlAs QDs, was focused on the sample surface using a microscope objective lens (×20, NA ~ 0.4). The QD emissions were collected by the same objective lens and detected by a triple grating spectrometer and a liquid N_2-cooled Si-CCD detector. The spectral resolution that determines the emission peak energies was ~5 μeV by the spectral fitting. In order to obtain the NSP transients by the time-resolved measurement, an electro-optic (EO) and an acousto-optic (AO) modulators were inserted into the excitation path and were used to produce the programmable pulse sequence with the arbitrary polarizations and pulse durations as shown later (Fig. 4).

Figure 1 shows the typical time-integrated PL spectra of a single InAlAs QD under a zero magnetic field. Note that the horizontal energy axis is replotted from the midpoint of the two PL peaks of a neutral exciton. From the various measurements,[8,9,13–17] the assignment of the spectral peaks could be achieved as follows: from the low energy side, a neutral biexciton (XX^0), a neutral exciton (X^0), and a positive trion (X^+). In our QD sample, X^+ PL was observed even at the minimum excitation power in the case of the wetting layer excitation. Also, the PL intensity was strongest for X^+ in the whole observed individual QDs. Therefore, we consider that our sample, which was grown under nominally undoped condition, is slightly p-doped.

X^0 PL shows a fine structure splitting of ~30 μeV due to the anisotropic exchange interaction, and therefore the states with the angular momenta ±1 are no longer eigenstates at 0 T. The exchange interaction plays no role on the ground state of XX^0, and X^+ states because they have spin-paired electrons or holes. Since XX^0 PL means the transition from XX^0 to X^0, the spectra show the same splitting (but inverse polarization) as that of X^0 PL spectra. X^+ and XX^0 have the binding energies of ~−1.85 meV and ~+2.57 meV, respectively,[18] which correspond to the calculated results obtained by quantum Monte Carlo methods[17,19] for a lens shaped QD with the diameter of ~17 nm and the height of ~5 nm.

The lowest X^+ state has the spin-paired two holes, which means that an electron of X^+ always has a hole available to recombine irrespective of its spin direction. In this sense, X^+ has no dark states and is different from X^0. Furthermore, the hole spin is easy to flip during the energy relaxation process from the wetting layer to the QD ground state. These features are advantageous to achieve the rapid NSP formation cycle compared to X^0 that has the dark states with a long lifetime. Therefore, in this InAlAs QD sample, X^+ is considered to contribute the NSP formation predominantly. In the later analysis, for simplicity, the system including X^+ and nuclei is considered.

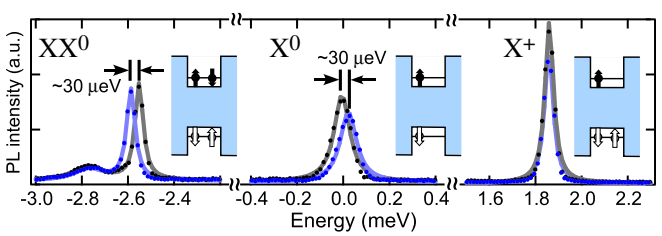

FIG. 1. Polarization selected PL spectra at 0 T. x (blue) and y (black) polarized spectra are depicted with the fitting curves of Lorentzian shape. Energy origin is shifted to the middle of the X^0 peaks, and the horizontal axis indicates the energy $\Delta E = E - E(X^0)$. For a good viewability, the vertical scale for X^+ is different from those for XX^0 and X^0, and the ratio of the observed peak PL intensities is ~1:1: ~3 for XX^0:X^0:X^+.

III. RESULTS AND DISCUSSION

A. Saturation of NSP and maximum Overhauser shift

In order to observe the transient OHS in the time-resolved PL measurement with high precision, it is necessary to prepare a distinct, reproducible, and highly stabilized NSP as an initial state for each measurement. First, we check the stability of the created NSP in upper and lower branches of the bistable response against the externally controllable parameters here.

As shown in the upper inset of Fig. 2(a), σ^- emission originates from the recombination of the spin-up electron (↑) and the spin-down hole (⇓), and the inverse spin combination (↓⇑) for the σ^+ emission in our definition. Thus, the transitions from the X^+ states with the spin configurations (↑⇓⇑ / ↓⇑⇓) to the hole states with the spins (⇑ / ⇓) generate σ^-/σ^+ polarized photons. The σ^- (σ^+) excitation generates the B_N in the opposite (same) direction to B_z. Hereafter, we focus on the σ^- case where the compensation of B_z via B_N is achieved, and consequently the bistability of NSP would occur.

Figure 2(a) shows the 2D plot of the external magnetic field dependence of X^+ PL spectra under σ^- excitation at 6 K; σ^+ and σ^- polarized PL peaks were taken sweeping B_z from 4 T to 5 T with the rate of +0.11 T/min. The difference energy ΔE_Z of two PL peaks is the sum of Zeeman splitting energies of the initial and final states as shown in the inset and is given as $\Delta E_Z = g_z^h \mu_B |B_z| + g_z^e \mu_B |B_z + B_N|$, where $g_z^{e(h)}$ and μ_B denote the electron (hole) g factor in the growth direction and Bohr magneton, respectively. It should be noted that the effect of B_N on the hole spin could be neglected except for the special case[20] due to its low probability of existence at the nucleus site. Since the electron and hole g factors of this QD are already known to be $g_z^e = -0.37$ and $g_z^h = +2.54$,[8] the electron Zeeman splitting energy E_Z^e can be deduced from the observed ΔE_Z as shown in Fig. 2(b). The difference energy between $E_Z^e(B_z)$ (denoted by the open circles) and $g_z^e \mu_B B_z$ (a thick dashed line) is attributed to the induced OHS. As shown in the figure, E_Z^e clearly indicates the abrupt reduction at ~4.3 T.

From the previous studies, it is known that the steady state of the averaged NSP $\langle I_z \rangle$ is the functions of three externally controllable parameters: the magnetic field B_z, the existence probability of an electron spin in a QD per unit time f_e, and the polarization degree of the localized electron spin $\langle S_z \rangle$. In fact, NSP in this InAlAs QD indicates the bistable response against B_z,[8] the excitation power,[9] and the

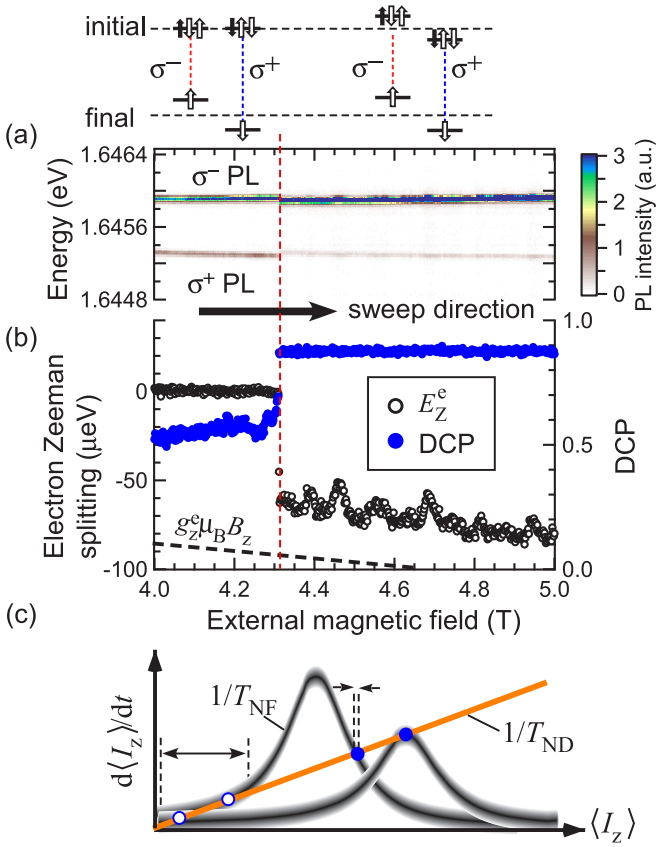

FIG. 2. (a) 2D image of X^+ PL spectra as a function of the external magnetic field. The data were taken by σ^--polarized excitation at 6 K sweeping the field from 4 T to 5 T with the rate of +0.11 T/min. The abrupt changes of OHS and DCP at ~4.3 T are observed clearly in the spectra. (b) The Zeeman splitting energy of the constituent electron states of X^+ and DCP (denoted by the open and closed circles) are plotted as a function of the external magnetic field. The electron Zeeman splitting only by the external field $g_z^e \mu_B B_z$ is indicated by a dashed line. The transition from high NSP state to the low NSP state is clearly observed at ~4.3 T. Inset: initial and final states of the transition and the relation between the spins and emission polarizations. (c) Simple schematic of the polarization ($1/T_{NF}$) and depolarization ($1/T_{ND}$) rates of NSP, and the observed NSP: a high NSP state (solid circle) and a low NSP state (open circle). In the Lorentzian-shaped polarization rate, the center and the amplitude are decided roughly by the magnitude of the external field and by the excitation power, respectively. The influence of the excitation power fluctuation on the polarization rate is depicted schematically as the gradation with a constant vertical width. The ranges of the accessible NSP induced by the $1/T_{NF}$ fluctuation for high and low NSP branches are indicated by the length of the arrows.

polarization of the excitation light.[9] Here, we focus on the stability of the high NSP state.

As seen in the figure, it is found that the high NSP state is more stabilized than the low NSP state. The observed NSP is determined by the balance of the polarization ($1/T_{NF}$) and the depolarization ($1/T_{ND}$) rates, and steadies down to the intersection points:[21] a high NSP state (solid circle) and a low NSP state (open circle) in Fig. 2(c). In the Lorentzian-shaped polarization rate, the center and the amplitude are decided roughly by the magnitude of the external field and by the excitation power, respectively. Although the excitation polarization and the external field can be controlled precisely and stably in our setup, it is difficult to suppress the fluctuation of the excitation power at present. This is mainly due to the deviation of the focusing by a microscope objective lens in a short time scale. The power fluctuation induces the change of the polarization rate as shown in Fig. 2(c), and correspondingly the steady state NSP also changes. In the figure, the effect of the fluctuation on the polarization rate is represented schematically as the gradation with a constant vertical width. Since the NSP polarization rate has the Lorentzian shape, the effect of the excitation power fluctuation on NSP is found to be larger for the low NSP state than for the high NSP state.

In addition, the saturations of the OHS as a function of the excitation power at fixed B_z were observed in the previous work.[9] Figure 3 shows the observed maximum OHS and the corresponding B_N^{max} as a function of B_z. According to the applied field B_z, the upper limit of the achieved OHS is determined. Therefore, the generated NSP near the maximum becomes stable under the sufficient excitation power, and this feature is feasible for providing the stable initial state.

In Fig. 2(b), the degree of circular polarization (DCP) is plotted also and the synchronized rapid change stands out. Here, the DCP is defined as $(I^- - I^+)/(I^- + I^+)$ ($I^{+(-)}$ denotes the integrated PL intensity of the $\sigma^{+(-)}$ component). From the figure, it is found clearly that, in the region of 4–4.3 T, the spin-up and down electron sublevels are almost degenerate, and the external field is canceled by B_N. The high NSP state changes suddenly to the low NSP state at the threshold field strength ~4.3 T. In the compensation region (4–4.3 T), the electron in a QD feels only the fluctuation ΔB_N of the frozen Overhauser field B_N,[22] and therefore the longitudinal component of the e-spin $\langle S_z \rangle$ shows the ensemble dephasing due to the transverse component of ΔB_N in a large number of the sampling measurements. In the outside of the compensation region, the electron in a QD feels the large longitudinal field ($>\Delta B_N$), and the effect of ΔB_N is suppressed. Therefore, the $\langle S_z \rangle$ returns to the almost initial value. In the detailed investigation of this interesting relation between DCP and OHS,[23] ΔB_N and the corresponding e-spin relaxation time ($=\hbar/(|g_e|\mu_B \Delta B_N)$) can be estimated to be ~40 mT and 0.75 ns (i.e., comparable to the exciton recombination time), respectively.

B. Depolarization process measurement

To observe the depolarization process of NSP, the erase-pump-probe method was employed. The experimental apparatus and the pulse sequence used in the measurements are shown in Fig. 4. The AO modulator connected to the arbitrary delay pulse generator controls the widths, intensities, and intervals of the pulse train, and the EO device controls the light polarizations. The pump pulse excites repeatedly a spin-selected electron in a target QD, and the NSP builds up due to its longer spin lifetime compared to electrons. The pump pulse continues to reach the saturated value of NSP mentioned in Sec. III A. The probe pulse is made shorter compared to the risetime of NSP to minimize its effect and samples the decay of NSP by measuring the OHS. The erase pulse with a linear polarization eliminates completely the residual NSP before the next pump pulse. As an example, the

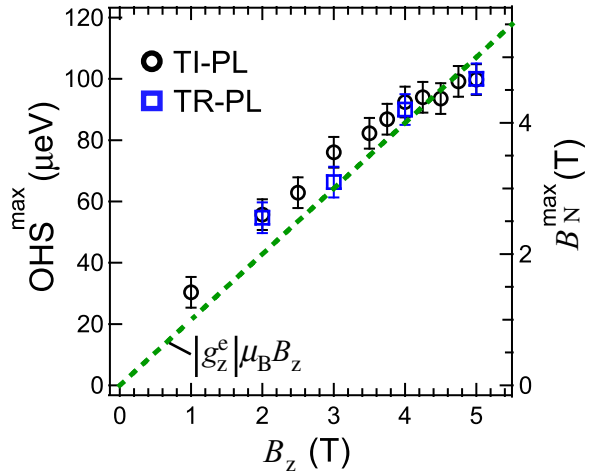

FIG. 3. The observed maximum OHS for σ^- excitation in time-integrated PL (TI-PL) and time-resolved PL (TR-PL) measurements is plotted as a function of the external field strength. The right axis indicates the maximum nuclear field that is converted by $B_N^{max} = |OHS^{max}/(g_z^e \mu_B)|$.

observed temporal behavior of NSP by the respective pulse is also shown in the bottom panel of Fig. 4(b).

Two main mechanisms are possible to induce NSP depolarization: the fluctuation of the hyperfine field produced by the electron spins (i.e., Knight field), and the spin diffusion out of the QD into the surrounding materials via the magnetic dipole-dipole interaction between nuclear spins. While NSP depolarization due to the magnetic dipole-dipole interaction is limited by the velocity of the spin transfer to the neighboring nucleus, the fluctuation of Knight field is effective with a large number of nuclear spins within the electron wave function. Therefore, the former mechanism, the fluctuation of Knight field, induces the more efficient NSP depolarization. Actually, Maletinsky *et al.* measured the decay time of NSP in both presence and absence of an electron spin by using a negative trion (X^-) in the charge tunable QD and demonstrated the fast decay of NSP in the order of a few ms in the presence of an electron in a QD

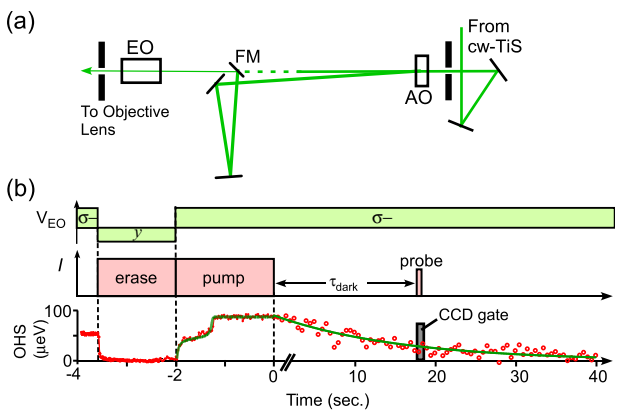

FIG. 4. (a) Experimental apparatus for the pulse intensity and polarization control. FM: flipper mirror, EO and AO: electro-optic and acousto-optic modulators, respectively. (b) Pulse sequence for the nuclear spin depolarization measurements. The light polarization controlled by applied voltage to EO modulator (upper panel), pulse intensity generated by AO modulator (middle panel), and an example of the temporal evolution of OHS and a CCD gate to probe the OHS (bottom panel).

under a zero and weak magnetic field.[24] In our measurements, the time interval between pump and probe pulses ($\tau_{dark} \geq 200$ ms) is enough longer than the exciton recombination time of the target InAlAs QD ($\tau_R \sim 0.75$ns) and no X^- is detected as shown in Fig. 1. In this condition, no electron can survive in the QD during τ_{dark} and consequently, the effect of the Knight field could be neglected. Therefore, the experimental data shown hereafter are considered to be mainly caused by the magnetic dipole-dipole interaction.

The dipolar coupling between two nuclear spins i and j can be written as

$$\hat{\mathcal{H}}_{dip} = \frac{K}{r_{ij}^3}\left(\hat{\boldsymbol{I}}^i \cdot \hat{\boldsymbol{I}}^j - 3\frac{(\hat{\boldsymbol{I}}^i \cdot \boldsymbol{r}_{ij})(\hat{\boldsymbol{I}}^j \cdot \boldsymbol{r}_{ij})}{r_{ij}^2}\right),$$

where $\hat{\boldsymbol{I}}^{i(j)}$ is the spin operator of the $i(j)$th nucleus, $\boldsymbol{r}_{ij}$ is the vector of length r_{ij} joining the two nuclei, and K is a coefficient including the permeability and gyromagnetic ratios of the two nuclei. The dipolar Hamiltonian of the total nuclear spin ensemble is then a sum over all nuclear spin pairs. The above Hamiltonian is commonly decomposed into the secular and non-secular parts. The former is composed of the terms which are proportional to $\hat{I}_z^i \hat{I}_z^j - \frac{1}{4}(\hat{I}_+^i \hat{I}_-^j + \hat{I}_-^i \hat{I}_+^j)$, where $\hat{I}_+^{i(j)}$ and $\hat{I}_-^{i(j)}$ are the raising and lowering operators of the $i(j)$th nuclear spin. The secular part is, therefore, spin-conserving and is responsible for diffusion and redistribution of the nuclear spins irrespective of the strength of B_z. In contrast, the non-secular part contains the terms which do not conserve the total spin and can contribute to the nuclear spin depolarization as far as $B_z \leq B_{dip}$, where B_{dip} is the local dipolar field. B_{dip} is the effective magnetic field generated on the site of a nucleus by its neighboring nuclear spins and characterizes the strength of the dipolar interaction $\hat{\mathcal{H}}_{dip}$. For bulk GaAs, B_{dip} is on the order of 0.1 mT.[25]

Figure 5(a) shows the NSP depolarization under $B_z = 4$ T at 6 K. The initial OHS of ~85 μeV was set to the maximum NSP at 4 T (see Fig. 3) by adjusting the intensity and width of the pump pulse. In Fig. 5(a), the dashed horizontal line indicates the OHS created only by the probe pulse. Making the trade-off between the S/N of the observed spectra and the influence of the probe pulse, the width (100 ms) and the intensity of the probe pulse were decided.

The diffusion of NSP can be calculated by the standard 3D diffusion equation $d\langle I_z\rangle/dt = D_{QD}\nabla^2\langle I_z\rangle$, where D_{QD} is a diffusion coefficient of QDs and is assumed to be time-independent and isotropic. By solving numerically the equation, the diffusion of NSP from QD into the barrier materials can be computed. For simplicity, we assumed that a QD is a box with the square base of 20 nm on a side and the height of 4 nm, and the in-plane anisotropy is also ignored in the calculation. Under the Gaussian distribution (FWHM of 20 nm in bottom plane and 4 nm in height, respectively) as the initial NSP, the depolarization due to the diffusion effect was computed as shown by the solid curves. To our best fitting, D_{QD} is estimated to be less than 5×10^{-15} cm^2/s. In addition, by using the relation $D_{QD} \sim d^2/T_{FF}$ (Ref. 1) (d is the distance between adjacent nuclei), the flip-flop time T_{FF} of

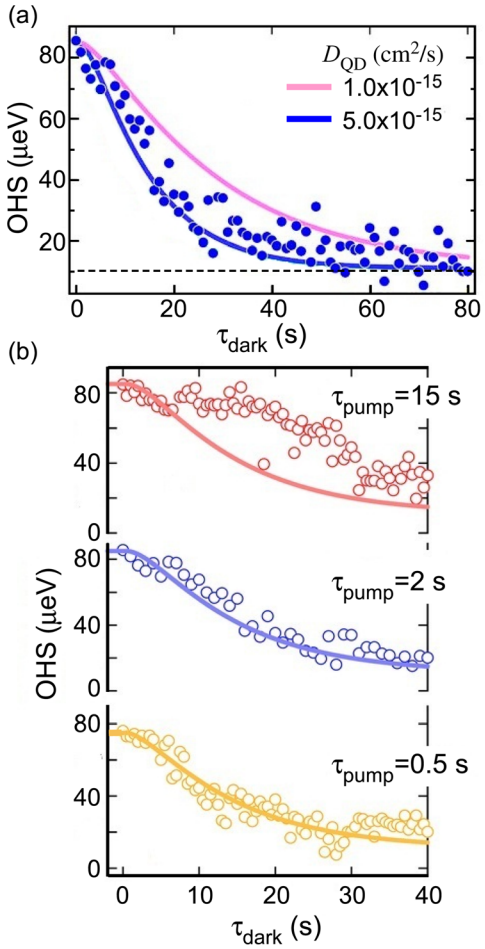

FIG. 5. (a) NSP relaxation due to spin diffusion at 4 T and 6 K. Closed circles show the OHS at σ^- pump pulse with $\tau_{pump} = 2$ s. The erase and probe pulse widths were set to $\tau_{erase} = 2$ s and $\tau_{probe} = 100$ ms. The solid lines indicate the calculated results of NSP diffusion in 3D diffusion model with some diffusion constants. (b) Pump duration dependence of the OHS decay. The results for the pump duration of 0.5, 2.0, and 15 s are plotted. The calculated curves by $D_{QD} = 5 \times 10^{-15}$ cm^2/s are also depicted for comparison.

nuclear spins can be roughly estimated to be ~350 ms for the nearest same nuclear species.

The obtained value of D_{QD} is 20 times smaller than that in bulk GaAs ($D_{bulk} \sim 10^{-13}$ cm^2/s)[26] and is of similar magnitude in self-assembled InGaAs QD ($D_{QD} \sim 5 \times 10^{-14}$ cm^2/s)[27] and interface-fluctuation GaAs QD ($D_{QD} \sim 2 \times 10^{-15}$ cm^2/s).[28] The spin diffusion is caused by the flip-flop between nuclear spins due to magnetic dipole-dipole interaction. Therefore, any energy mismatch between the associated nuclear states can slow down the mutual spin flip process. Dipolar and quadrupolar disorders in alloy and nuclear site-dependent quadrupolar energy shift due to strain are likely to suppress the spin transfer for the case of no electron residence in a QD.

The calculated results depend on the broadening of the initial NSP created by the pump pulse. In order to confirm the effect of the initial NSP broadening, the dependence on the pump pulse duration was measured as shown in Fig. 5(b). The pump pulse duration τ_{pump} was changed from 0.5 s to 15 s, and the decay of OHS was measured. In increasing the τ_{pump}, the start of the OHS decay was found to be delayed and the initial constant OHS part was prolonged. For the easy-to-see comparison, the calculated curve for $D_{QD} = 5 \times 10^{-15}$ cm^2/s was overlaid on the respective measured result. The result for the longer pump pulse deviates from the simple calculation. This strongly suggests the NSP in the QD surroundings, which would be generated during the τ_{pump}, suppresses the spin transfer from QD region. The similar time lag of the OHS decay was observed decreasing the magnetic field in the case of the constant pump condition (constant τ_{pump} and intensity). The maximally achievable OHS depends on the applied magnetic field as shown in Fig. 3, and therefore, under the constant pump condition, the NSP in the QD surroundings generated during τ_{pump} increases in decreasing the applied field. Such a magnetic field dependence of NSP depolarization also supports the above estimation.

Finally, the influence of resident hole on nuclear spin depolarization is discussed briefly. As mentioned above, nuclear spin depolarization is induced by the fluctuation of Knight field and the spin diffusion via the magnetic dipolar interaction between nuclei. The hyperfine interaction, which is the spin exchange between the electron (hole) and the nuclei, can be decomposed into the following two terms: the Fermi's contact term and the dipolar term. While the contact term is mainly contributed by an electron due to the large existence probability at the nucleus site, the dipolar term is dominated by a hole spin with the angular momentum $l = 1$. There are a few elaborate works about the influence of a confined electron in a QD on the nuclear spin depolarization.[24,29] In the case that only an electron exists in the QD region, which can be realized after the X^- emission, the contact term contributes dominantly to the nuclear spin depolarization, because it is much stronger than the other depolarization terms. Latta *et al.* revealed that the resident electron causes the nuclear spin depolarization via the hyperfine-mediated indirect nuclear spin interaction and the cotunneling mediated nuclear spin flips.[29] Being similar to the case of a resident electron, the resident hole has the possibility to affect the nuclear spin depolarization via the dipolar term of hyperfine interaction. In general, the hyperfine constant of the dipolar term is more than one order of magnitude smaller than that of the contact term.[20] In addition, the dipolar hyperfine interaction is highly anisotropic for pure heavy hole and the efficiency relies on the large hh-lh mixing.[20,30] According to the high DCP of X^+-PL (~0.9) as shown in Fig. 2(b), the degree of hh-lh mixing is considered to be low in our sample. In addition, the decay time of Overhauser field is nearly same as the decay time (~60 s.) in the case that no particles exist in a QD.[24] Those facts suggest that the resident hole has small influence on the nuclear spin depolarization.

IV. SUMMARY

In summary, we performed the time-resolved measurements of the nuclear spin depolarization processes in a single InAlAs QD by using the erase-pump-probe technique. Compared with the standard 3D diffusion model, the diffusion coefficient of a target single $In_{0.75}Al_{0.25}$ As QD can be estimated less than $\sim 5 \times 10^{-15}$ cm^2/s, which is one order magnitude smaller than that in bulk GaAs and is the similar

magnitude in other experimental results of QDs. The slow transfer of the spin energy is considered to be due to the dipole-dipole interaction of the nuclei, and the pump duration dependence suggests strongly that the NSP in QD surroundings suppresses the spin transfer from the QD region.

ACKNOWLEDGMENTS

We acknowledge H. Sasakura for fruitful discussions. This work was supported in part by the Grant-in-Aid for Scientific Research (Grant No. 22310063) from the Ministry of Education, Culture, Sports, Science, and Technology, Japan.

[1]*Optical Orientation*, Modern Problems in Condensed Matter Sciences, edited by F. Meier and B. Zakharchenya (North-Holland, New York, 1984), Vol. 8, Chaps. 2 and 5.
[2]A. Abragam, *The Principles of Nuclear Magnetism* (Clarendon, Oxford, 1961).
[3]D. Gammon, Al. L. Efros, T. A. Kennedy, M. Rosen, D. S. Katzer, D. Park, S. W. Brown, V. L. Korenev, and I. A. Merkulov, Phys. Rev. Lett. **86**, 5176 (2001).
[4]T. Yokoi, S. Adachi, H. Sasakura, S. Muto, H. Z. Song, T. Usuki, and S. Hirose, Phys. Rev. B **71**, R041307 (2005).
[5]P.-F. Braun, B. Urbaszek, T. Amand, X. Marie, O. Krebs, B. Eble, A. Lemaitre, and P. Voisin, Phys. Rev. B **74**, 245306 (2006).
[6]A. I. Tartakovskii, T. Wright, A. Russell, V. I. Falko, A. B. Van'kov, J. Skiba-Szymanska, I. Drouzas, R. S. Kolodka, M. S. Skolnick, P. W. Fry, A. Tahraoui, H.-Y. Liu, and M. Hopkinson, Phys. Rev. Lett. **98**, 026806 (2007).
[7]P. Maletinsky, C. W. Lai, A. Badolato, and A. Imamoglu, Phys. Rev. B **75**, 035409 (2007).
[8]R. Kaji, S. Adachi, H. Sasakura, and S. Muto, Appl. Phys. Lett. **91**, 261904 (2007).
[9]R. Kaji, S. Adachi, H. Sasakura, and S. Muto, Phys. Rev. B **77**, 115345 (2008).
[10]E. A. Chekhovich, M. N. Makhonin, J. Skiba-Szymanska, A. B. Krysa, V. D. Kulakovskii, M. S. Skolnick, and A. I. Tartakovskii, Phys. Rev. B **81**, 245308 (2010).
[11]J. M. Taylor, C. M. Marcus, and M. D. Lukin, Phys. Rev. Lett. **90**, 206803 (2003).
[12]S. Muto, S. Adachi, T. Yokoi, H. Sasakura, and I. Suemune, Appl. Phys. Lett. **87**, 112506 (2005).
[13]H. Kumano, S. Kimura, M. Endo, H. Sasakura, S. Adachi, S. Muto, and I. Suemune, J. Nanoelectron. Optoelectron. **1**, 39–51 (2006).
[14]R. Kaji, K. Yamada, H. Sasakura, and S. Adachi, Phys. Status Solidi B **245**, 2662–2666 (2008).
[15]S. Adachi, N. Yatsu, R. Kaji, and S. Muto, Appl. Phys. Lett. **91**, 161910 (2007).
[16]R. Kaji, S. Adachi, T. Shindo, and S. Muto, Phys. Rev. B **80**, 235334 (2009).
[17]R. Kaji, Doctoral thesis, Hokkaido University, 2011.
[18]Here, the binding energies are defined by $E_b(X^+) = E(X^0) - E(X^+)$ and $E_b(XX^0) = 2E(X^0) - E(XX^0)$.
[19]T. Tsuchiya, Physica E **7**, 470–474 (2000).
[20]B. Eble, C. Testelin, P. Desfonds, F. Bernardot, A. Balocchi, T. Amand, A. Miard, A. Lemaître, X. Marie, and M. Chamarro, Phys. Rev. Lett. **102**, 146601 (2009).
[21]*Spin Physics in Semiconductors*, Springer Series in Solid-State Sciences, edited by M. I. Dyakonov (Springer-Verlag, Berlin/Heidelberg, 2008), Vol. 157, Chap. 11.
[22]I. A. Merkulov, Al. L. Efros, and M. Rosen, Phys. Rev. B **65**, 205309 (2002).
[23]R. Kaji, S. Adachi, H. Sasakura, and S. Muto, Phys. Rev. B **85**, 155315 (2012).
[24]P. Maletinsky, A. Badolato, and A. Imamoglu, Phys. Rev. Lett. **99**, 056804 (2007).
[25]D. Paget, G. Lampel, B. Sapoval, and V. I. Safarov, Phys. Rev. B **15**, 5780 (1977).
[26]D. Paget, Phys. Rev. B **25**, 4444 (1982).
[27]M. N. Makhonin, A. I. Tartakovskii, A. B. Vankov, I. Drouzas, T. Wright, J. Skiba-Szymanska, A. Russell, V. I. Fal'ko, M. S. Skolnick, H.-Y. Liu, and M. Hopkinson, Phys. Rev. B **77**, 125307 (2008).
[28]A. E. Nikolaenko, E. A. Chekhovich, M. N. Makhonin, I. W. Drouzas, A. B. Van'kov, J. Skiba-Szymanska, M. S. Skolnick, P. Senellart, D. Martrou, A. Lemaitre, and A. I. Tartakovskii, Phys. Rev. B **79**, 081303(R) (2009).
[29]C. Latta, A. Srivastava, and A. Imamoglu, Phys. Rev. Lett. **107**, 167401 (2011).
[30]C. Testelin, F. Bernardot, B. Eble, and M. Chamarro, Phys. Rev. B **79**, 195440 (2009).